CHEMISTRY
A EUROPEAN JOURNAL

DOI: 10.1002/chem.200700559

Artificial DNAs Based on Alkynyl *C*-Nucleosides as a Superior Scaffold for Homo- and Heteroexcimer Emissions

Junya Chiba,[a] Sakiko Takeshima,[a] Kikyo Mishima,[a] Hajime Maeda,[b] Yasuaki Nanai,[b] Kazuhiko Mizuno,[b] and Masahiko Inouye*[a]

In memory of Professor Yoshihiko Ito

Abstract: DNA-like fluorescent oligomers composed of alkynyl β-D-ribofuranosides bearing pyrene, perylene, and anthracene as a fluorophore were synthesized by solid-phase DNA synthesis. The fluorescent oligomers possess the defined number and order of the fluorophores. In these oligomers, the adjacent fluorophores efficiently interact with each other by hydrophobic interactions in their electronic ground states in a face-to-face fashion. The predominant excimer emissions were observed from not only the homooligomers (pyrene–pyrene and perylene–perylene systems) but also the heterooligomers (pyrene–perylene, pyrene–anthracene, and perylene–anthracene systems) in aqueous media.

Keywords: artificial DNA · excimers · fluorescence · nucleosides · photochemistry

Introduction

Emissions from homo- and heteroexcimers of polycyclic aromatic hydrocarbons have long been attractive in terms of their inherent and novel luminescent features. Inspiring researchers in its own right, the photophysics of the emission has been investigated in detail to elucidate the radiation and nonradiation processes from the excimers.[1] Generally, excimer emission is observed only in highly concentrated solutions because the formation of an excimer requires the encounter of one electronically excited fluorophore with another, usually that of the ground state, in an extremely short time. To make fluorophores interact with each other in low concentrations suitable for quantitative experiments, intramolecular strategies have been adopted by covalently connecting two or more fluorescent moieties.[2–4] The examples include simple molecules possessing multiple fluorophores with the aid of appropriate linkers,[2] fluorophore-attached polymers as a pendant style,[3] and macrocycles such as cyclophanes containing fluorophores as a core.[4] Although these approaches are valid for obtaining photophysical data of the excimers, their syntheses are time-consuming and lack the generality for introducing various fluorophores into the skeletons at will.

The excimer formation has also been utilized for solving critical problems of biological events. The conventional illustrations are concerned with protein–substrate and protein–protein interactions,[5] hybridizations and conformational changes of DNAs and RNAs,[6] and real-time dynamics of cell membranes.[7] Recently, excimer-forming molecules have been employed as a fluorescent tag for labeling biomolecules.[6a,c,d,8] In the labeling experiments, these tags, strongly lipophilic aromatic hydrocarbons, must be applied under biological conditions, such as in aqueous buffer media. This sometimes causes technical problems, especially in the case of highly condensed tags with wider polyaromatic hydrocarbons.

Kool and co-workers have reported their original strategy for creating fluorescent tags by replacing DNA bases of oligonucleotides with various fluorescence molecules.[9] In this combinatorial manner for the DNA-like fluorescent oligomers, a DNA synthesizer allows easy preparations of the oligomers with the defined number and order of the fluoro-

[a] Dr. J. Chiba, S. Takeshima, K. Mishima, Prof. Dr. M. Inouye
Graduate School of Pharmaceutical Sciences
University of Toyama
Sugitani 2630, Toyama 930–0194 (Japan)
Fax: (+81) 76-434-5049
E-mail: inouye@pha.u-toyama.ac.jp

[b] Dr. H. Maeda, Y. Nanai, Prof. Dr. K. Mizuno
Department of Applied Chemistry
Graduate School of Engineering
Osaka Prefecture University
Gakuen-cho 1–1, Sakai, Osaka 599–8531 (Japan)

Supporting information for this article is available on the WWW under http://www.chemeurj.org/ or from the author.

phores. Indeed, they synthesized a tetrameric fluorophore library composed of more than 14,000 members on beads, and observed the multicolor emissions at once in aqueous media. For synthetic convenience of the library, they used a mixture of the α and β anomers of the fluorescent nucleoside analogues as a monomer, in which non-natural α anomers are major components. Because of this structural diversity, however, the detailed photophysical properties remain to be investigated from the viewpoint of the specific radiation from the multiply interacting individual tetrameric fluorophore.[9c]

To clarify each emissive characteristic from such fluorescent oligomers, chemical structures in the oligomers must be well defined. Therefore, all of the anomeric configurations in the oligomer should be the same, hopefully being β anomers of natural nucleosides, as the conformation of the oligomer can be easily speculated. We previously reported the stereoselective synthesis of alkynyl *C*-2-deoxy-β-D-ribofuranosides as a versatile building block for many different kinds of *C*-nucleotides.[10] By means of the synthetic usefulness of the acetylenic function, a variety of fluorophores such as pyrene, perylene, and anthracene will be attached to the deoxyribose through an acetylenic bond in high yields with the β configuration. Here we report the synthesis and detailed photophysical data of the fluorescent oligomers composed of the alkynyl β-D-ribofuranosides (Scheme 1).

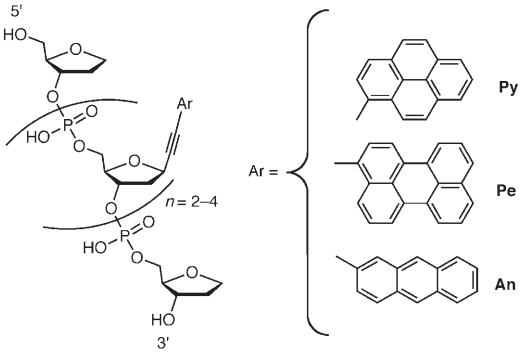

Scheme 1. Chemical structure of DNA-like fluorescent oligomers based on alkynyl *C*-nucleosides.

This novel DNA-like skeleton provides a superior scaffold for investigating homo- and heteroexcimer formation and its radiation in aqueous media, and the results presented here can be expected to lead to fruitful applications in biological sciences.

Results and Discussion

Structure of fluorescent oligomers: Pyrene, perylene, and anthracene were chosen as representative fluorophores. Each of the fluorophore-attached β-D-ribofuranosides is oligomerized by solid-phase DNA synthesis. Therefore, the DNA-like fluorescent oligomers possess not only the defined number and order of the fluorophores but also the same β configurations at all of their anomeric positions. Water solubility of the oligomers is provided from the negative charges of the phosphodiester backbone. Even in diluted aqueous solutions, the adjacent hydrophobic fluorophores in the oligomers would interact with each other adequately to adopt suitable conformations in their electronic ground states. This motion may be assisted by puckering flexibilities of the deoxyribose and by an additional hydrophobicity of the acetylenic bond in the alkynyl *C*-nucleosides.

Synthesis and abbreviation of oligomers: DMTr-protected fluorescent nucleoside analogues **4** were prepared by Sonogashira coupling of bromohydrocarbons with **3** derivatized from the published **1** (Scheme 2).[10] The analogues **4** were

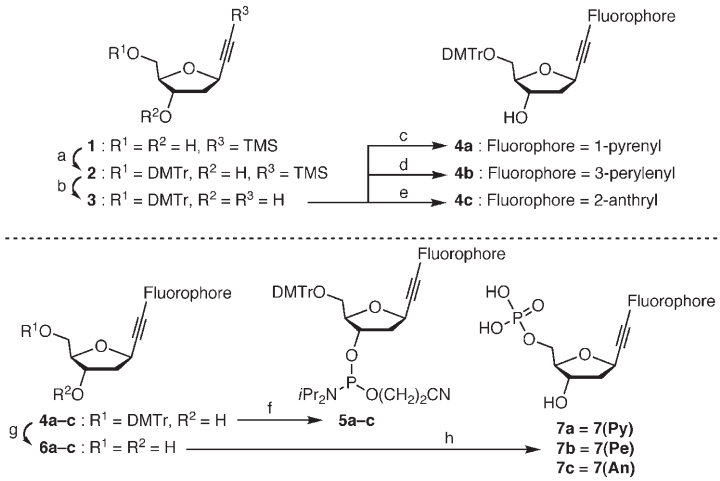

Scheme 2. a) 4,4′-Dimethoxytrityl chloride, 4-(*N*,*N*-dimethylamino)pyridine, pyridine; b) nBu_4NF, H_2O, THF; c) 1-bromopyrene, $[Pd(PPh_3)_4]$, CuI, iPr_2NH, THF; d) 3-bromoperylene, $[Pd(PPh_3)_4]$, CuI, iPr_2NH, THF; e) 2-bromoanthracene, $[Pd(PPh_3)_4]$, CuI, iPr_2NH, THF; f) NC-$(CH_2)_2OPClN(iPr)_2$, iPr_2NEt, CH_2Cl_2; g) *p*-toluenesulfonic acid monohydrate, CH_2Cl_2; h) phosphorus oxychloride, dioxane, pyridine.

converted into the corresponding phosphoramidites **5** and also into 5′-monophosphate derivatives **7** as reference water-soluble monomers (see Supporting Information). The phosphoramidites **5** were then subjected to automated DNA synthesis to give fluorescent oligomers on a solid support. After having been released from the support, the oligomers were purified by reverse-phase HPLC and characterized by MALDI-TOF mass spectrometry (see Experimental Section). In the sequence of the oligomers, the pseudonucleoside residues containing pyrene, perylene, and anthracene are abbreviated as **Py**, **Pe**, and **An**, respectively. An abasic nucleoside residue is abbreviated as **ab**, and this was introduced into both the ends of the sequence to improve the water solubility of the oligomers. The oligomer referred to as **ab-Py-Pe-ab**, for instance, possesses the abasic, pyrene-attached, perylene-attached, and abasic nucleoside residues from 5′ (the left end) to 3′ (the right end) of the sequence,

and the "hyphen" indicates a phosphodiester bond. Table 1 shows the oligomers examined in this study.

Table 1. Photophysical data for fluorophore-linked monomers and oligomers.

Monomers and oligomers	Absorption[a] λ_{abs}[b] [nm]	$\varepsilon \times 10^4$ [$mol^{-1}\,dm^3\,cm^{-1}$]	Fluorescence λ_{em}[a,c,d] [nm]	Φ_f[a,e]	τ_s[f] [ns]
7(Py)	360	5.41	385[c]	0.66	35.1
ab-Py-Py-ab	365	3.62	510[d]		29.3, 66.8
ab-Py-Py-Py-ab	364	4.99	521[d]		30.6, 75.1
ab-Py-Py-Py-Py-ab	365	5.80	515[d]		28.0, 86.5
7(Pe)	454	2.70	468[c]	0.66	4.35
ab-Pe-Pe-ab	462	3.23	595[d]		4.42, 14.2
7(An)	387	0.47	398[c]	0.37	6.06
ab-An-An-ab	391	0.80	525[d]		6.81
ab-Py-Pe-ab	464	2.48	522[d]		7.88, 16.2
ab-Py-Pe-Py-ab	469	1.83	517[d]		_[g]
ab-Py-An-ab	365	1.95	500[d]		73.0, 104
ab-Pe-An-ab	461	2.80	526[d]		18.1, 28.8

[a] **[7(Py)]** = **[7(Pe)]** = **[7(An)]** = **[ab-Py-Pe-ab]** = **[ab-Py-Pe-Py-ab]** = **[ab-Py-An-ab]** = **[ab-Pe-An-ab]** = 2.0×10^{-5} M, **[ab-Py-Py-ab]** = **[ab-Pe-Pe-ab]** = **[ab-An-An-ab]** = 1.0×10^{-5} M, **[ab-Py-Py-Py-ab]** = 6.7×10^{-6} M, **[ab-Py-Py-Py-Py-ab]** = 5.0×10^{-6} M in H_2O, degassed by bubbling of Ar. [b] λ_{abs} is the absorption band appearing at the longest wavelength. [c] λ_{em} is the fluorescence band appearing at the shortest wavelength. [d] λ_{em} is the excimer fluorescence band. [e] Fluorescence quantum yields of the monomers in H_2O, degassed by bubbling of Ar, measured at RT. Standards used were 9,10-diphenylanthracene (for **7(Py)** and **7(An)**) and perylene (for **7(Pe)**), OD < 0.02. Φ_f(9,10-diphenylanthracene) = 0.95 in EtOH.[17] Φ_f(perylene) = 0.92 in EtOH.[18] [f] Fluorescence lifetime in aerated H_2O (5.0×10^{-6} M). [g] Not determined.

Photophysical properties of pyrene-linked homooligomers: To elucidate the luminescent property of each individual oligomer, all photophysical measurements must be carried out below this concentration so that the intermolecular association of the oligomer is negligible. Therefore, intermolecular association tendencies of the oligomers were studied in advance with **ab-Py-Py-ab** and **ab-Pe-Pe-ab**. The absorption spectra of these representative oligomers were measured in water at room temperature. The shapes of the spectra are not sensitive to their concentrations, and at $\leq 1.0\times10^{-4}$ M, the absorbances of these oligomers fit in proportion to the concentration obeying Beer's law. Thus, the contribution of the intermolecular association of the oligomers can be ruled out below that concentration. Taking this fact into account, the following measurements were conducted.

First, a series of homooligomers with the pyrene residues were chosen because pyrene is an well-known fluorophore that readily exhibits excimer emission.[11] Figure 1A shows the absorption spectra of the pyrene-linked monomer **7(Py)** and homooligomers, **ab-Py-Py-ab**, **ab-Py-Py-Py-ab**, and **ab-Py-Py-Py-Py-ab**. For an easy comparison of the spectroscopic data, the concentration of each solution was normalized against the chromophore concentration [**Py**]. The absorption maximum of **7(Py)** appeared at 360 nm, and its shape and absorption coefficient (ε) are very similar to those of the simple monoalkynylpyrenes in our previous report.[12] However, as the number of the pyrene residues in the oligomers increased, we observed significant hypochromism and small red-shifts of the absorption bands with the broadening. Peak-to-valley ratio (P_A) was used to estimate the degree of the π–π interaction between chromophores.[13] The value is calculated by using the equation $P_A = A^{peak}/A^{valley}$, in which A^{peak} is for the absorption intensity of the band appearing at the longest wavelength and A^{valley} for that of the valley between the longest wavelength band and the adjacent one. The P_A values of the oligomers are 1.13, 1.10, and 1.11 for **ab-Py-Py-ab**, **ab-Py-Py-Py-ab**, and **ab-Py-Py-Py-Py-ab**, respectively. The values are considerably smaller than P_A = 2.07 of **7(Py)**, indicating strong face-to-face interactions for the pyrene residues of the oligomers in their ground states.

The steady-state fluorescence spectra of the pyrene-linked monomer and homooligomers were measured in degassed water (Figure 1B). The monomer **7(Py)** revealed a characteristic monomeric fluorescence with emission maxima at 385 and 405 nm. The fluorescence quantum yield (Φ_f) of **7(Py)** is 0.66, comparable to those of the simple alkynylpyrenes.[12] The emission maxima depended on the concentration: at $\geq 1.0\times10^{-4}$ M, a new emission (λ_{max} = 507 nm) that was thought to be for an intermolecular excimer appeared (Supporting Information Figure S1). On the other hand, the oligomers (**ab-Py-Py-ab**, **ab-Py-Py-Py-ab**, and **ab-Py-Py-Py-Py-ab**) exhibited broad and structureless emissions at around 510 nm nearly without the monomer emissions. The wavelengths of the emission maxima of the oligomers were independent of their concentrations, so that the emissions

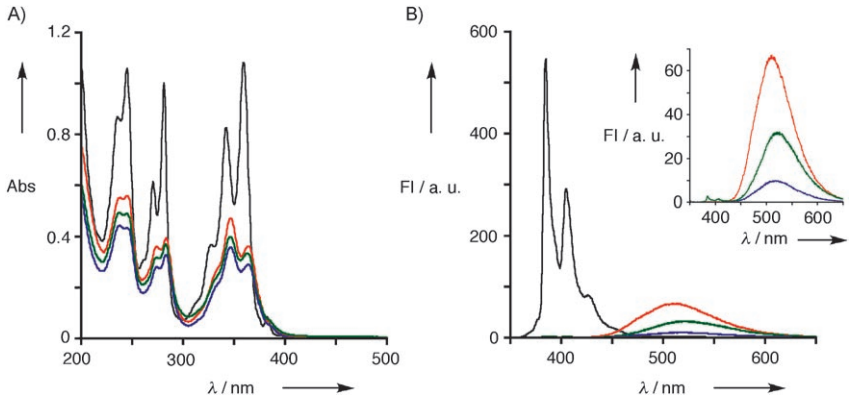

Figure 1. Absorption (A) and fluorescence (B) spectra of **7(Py)** (black line), **ab-Py-Py-ab** (red line), **ab-Py-Py-Py-ab** (green line), and **ab-Py-Py-Py-Py-ab** (violet line) in H_2O at 25 °C (FI = fluorescence intensity). Concentrations: **[7(Py)]** = 2.0×10^{-5} M, **[ab-Py-Py-ab]** = 1.0×10^{-5} M, **[ab-Py-Py-Py-ab]** = 6.7×10^{-6} M, and **[ab-Py-Py-Py-Py-ab]** = 5.0×10^{-6} M. Excitation wavelength is 350 nm. The inset expands the region of the excimer emission.

must result from the intramolecular interactions between the pyrene residues. The emissions should be radiated from so-called "static excimers", as in water the tethered pyrene residues interact with each other in their ground states, as mentioned above.[13] The excimer emissions of the oligomers gradually decreased as the number of the pyrenes increased, apparently being due to the self-quenching of the excimers. Although in the trimer and tetramer, triply π, π, π stacking or higher coordinations of the pyrene residues might be possible, an extra emission band from such higher coordinations could not be found. Nevertheless, on the basis of these data, our artificial DNA-like skeleton is demonstrated to be a superior scaffold giving excimer emissions of tethered fluorophores in water.

Photophysical properties of perylene- and anthracene-linked homooligomers: Next, perylene was introduced into the alkynyl *C*-nucleosides because excimer emissions of perylene are rare in solutions. Figure 2A displays absorption spectra of the perylene-linked monomer **7**(**Pe**) and homodimer **ab-Pe-Pe-ab** under the same conditions as described for the pyrene-linked ones. The monomer **7**(**Pe**) has an absorption maximum at 454 nm and its absorption coefficient is $\varepsilon = 2.70 \times 10^4\ mol^{-1}\,dm^3\,cm^{-1}$, so that it exists as an intensely colored orange–red solid. Substantial hypochromism and small red-shift of the longest wavelength band were observed with the broadening also in the case of **ab-Pe-Pe-ab**. The P_A values of **7**(**Pe**) and **ab-Pe-Pe-ab** are 1.63 and 1.21, respectively, suggesting that the perylene residues in **ab-Pe-Pe-ab** interact with each other in a manner similar to those of the pyrene-linked oligomers.

During recording of the fluorescence measurements of **7**(**Pe**) and **ab-Pe-Pe-ab**, special care was taken in the preparation of the sample solutions to avoid them being exposed to light. Thus, the spectra were recorded as soon as the sample was available (Figure 2B).[14] The monomer **7**(**Pe**) emitted a characteristic monomeric fluorescence with emission maxima at 468 and 495 nm, and its Φ_f value is 0.66. On the other hand, the dimer **ab-Pe-Pe-ab** predominantly gave a broad and structureless emission band at around 600 nm, which even tailed to 800 nm. The emission should radiate from the intramolecular perylene excimer by analogy with the pyrene-type oligomers. Although perylene is known to show the excimer emission in its crystalline form,[15] little is known for the emission in solutions, especially in diluted media.[9c,16] By use of the present strategy, the excimer emission of **ab-Pe-Pe-ab** could be detected at concentrations as low as approximately 1.0×10^{-7} M. These findings demonstrate the superiority of our scaffold to realize excimer emissions of various fluorophores.

Unfortunately, we observed only a weak excimer emission for the anthracene dimer **ab-An-An-ab** in the fluorescence spectrum (Figure 3). In **ab-An-An-ab**, the adjacent anthracene residues overlapped each other insufficiently because of a comparatively narrow plane of the anthracene ring (see the following section on heterooligomers). This speculation is suggested by the fact that the absorption spectrum of **ab-An-An-ab** scarcely changed compared to that of the monomer **7**(**An**) with respect to the hypochromism, red-shifts, and broadening of the bands within the wavelength region of 300–400 nm.

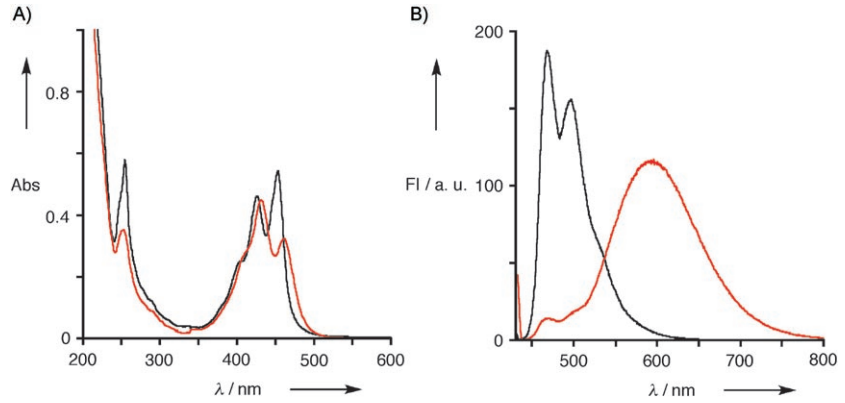

Figure 2. Absorption (A) and fluorescence (B) spectra of **7**(**Pe**) (black line) and **ab-Pe-Pe-ab** (red line) in H_2O at 25 °C (FI = fluorescence intensity). Concentrations: [**7**(**Pe**)] = 2.0×10^{-5} M, [**ab-Pe-Pe-ab**] = 1.0×10^{-5} M. Excitation wavelength is 430 nm.

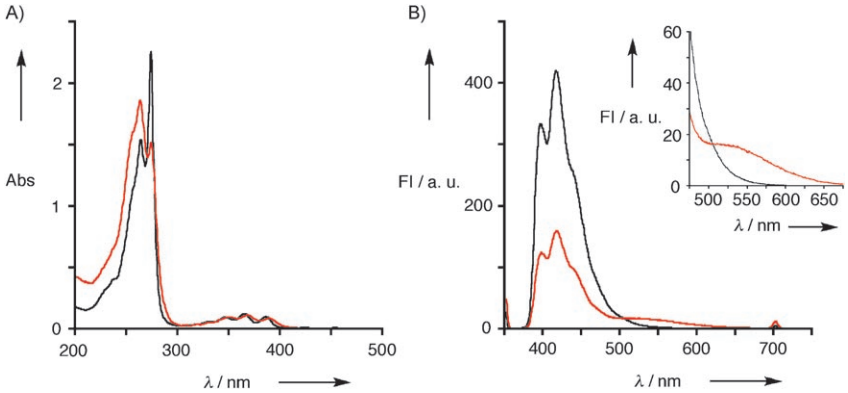

Figure 3. Absorption (A) and fluorescence (B) spectra of **7**(**An**) (black line) and **ab-An-An-ab** (red line) in H_2O at 25 °C (FI = fluorescence intensity). Concentrations: [**7**(**An**)] = 2.0×10^{-5} M, [**ab-An-An-ab**] = 1.0×10^{-5} M. Excitation wavelength is 350 nm. The inset expands the region of the excimer emission.

Photophysical properties of heterooligomers: Because the homooligomers showed distinct excimer emissions, we then examined heterooligomers consisting of different kinds of polycyclic aromatic hydrocarbons. We chose **ab-Py-Pe-ab**, **ab-Py-An-ab**, and **ab-Pe-An-ab** as sequences for this purpose. The concentration of all heterooligomers is 2.0×10^{-5} M, so that each of the chromophore residues **Py**, **Pe**, and **An** exists at the same concentration. In the absorption spectrum of **ab-Py-Pe-ab**, substantial red-shifts were observed within the wavelength region corresponding to the absorption bands for the perylene residue (400–500 nm). On the other hand, the corresponding bands for the pyrene residue (300–400 nm) shifted largely hypochromically (Figure 4A). Such red-shifts and hypochromism were observed also in the cases of **ab-Py-An-ab** and **ab-Pe-An-ab**, however, the exact degree of hypochromism of these two spectra could hardly be evaluated because of the overlap between the chromophore residues (Figure S2). The chromophores in the heterooligomers were found to intramolecularly interact with each other, as in the cases of the homooligomers.

The fluorescence spectrum of **ab-Py-Pe-ab** exhibited a broad emission at around 522 nm, almost without both of the monomer emissions from the pyrene and perylene residues (Figure 4B, see also Figure S3). The emission maximum is located between those of the pyrene excimer (510 nm, Figure 1B) and the perylene excimer (595 nm, Figure 2B). The emission spectra are almost the same when the oligomer is excited at 350 and 430 nm, corresponding to the absorption regions of the pyrene and perylene chromophores, respectively (Figure S3). Moreover, the excitation spectrum monitored at 520 nm is structurally analogous to the absorption spectrum of **ab-Py-Pe-ab** (Figure S4 A). On the basis of these data, the emission proved to radiate from the heteroexcimers consisting of the pyrene and perylene residues, and not to be due to fluorescence resonance energy transfer (FRET). Strikingly similar heteroexcimer emission was seen in **ab-Py-Pe-Py-ab**, however, no characteristic emission from triplex coordinations of the fluorophores was monitored in this oligomer (Figure S5).

In contrast to **ab-An-An-ab**, the anthracene-linked heterooligomers revealed fluorescent properties similar to those for **ab-Py-Pe-ab**. Therefore, in the fluorescence spectra, **ab-Py-An-ab** and **ab-Pe-An-ab** have broad peaks at around 500 and 525 nm, respectively (Figure 4C and D). These emissions must result from the heteroexcimer of the pyrene or perylene residue with anthracene, as evidenced by the similarity between the excitation and absorption spectra of these oligomers (Figure S4B, C). In these heterooligomers, the anthracene residue exists close to the wider aromatic hydrocarbons of pyrene and perylene rather than anthracene itself, as in the case of **ab-An-An-ab**. This situation is most likely to be responsible for the effective excimer formation in the anthracene-linked heterooligomers. To the best of our knowledge, these are first examples for the predominant emission from heteroexcimers of anthracenes.

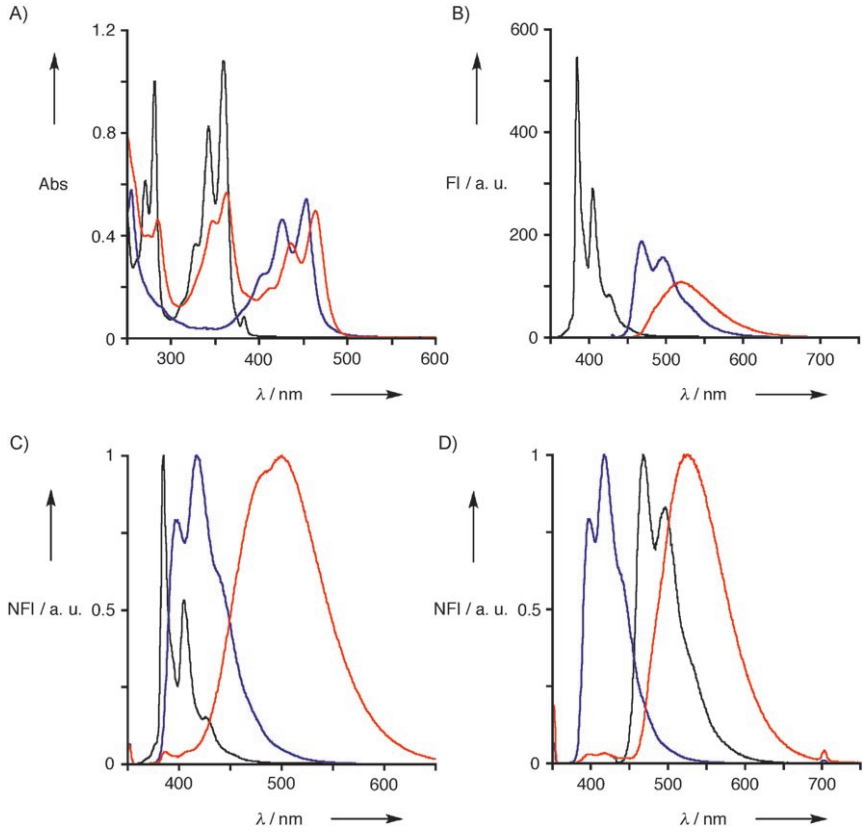

Figure 4. A and B: Absorption (A) and fluorescence (B) spectra of **7(Py)** ($\lambda_{ex}=350$ nm, black line), **7(Pe)** ($\lambda_{ex}=430$ nm, violet line), and **ab-Py-Pe-ab** ($\lambda_{ex}=350$ nm, red line) in H_2O at 25 °C (FI = fluorescence intensity). C and D: Normalized fluorescence spectra of (C) **7(Py)** ($\lambda_{ex}=350$ nm, black line), **7(An)** ($\lambda_{ex}=350$ nm, violet line) and **ab-Py-An-ab** ($\lambda_{ex}=350$ nm, red line); (D) **7(Pe)** ($\lambda_{ex}=430$ nm, black line), **7(An)** ($\lambda_{ex}=350$ nm, violet line), and **ab-Pe-An-ab** ($\lambda_{ex}=350$ nm, red line) in H_2O at 25 °C (NFI = normalized fluorescence intensity). Concentrations: [**7(Py)**] = [**7(Pe)**] = [**7(An)**] = [**ab-Py-Pe-ab**] = [**ab-Py-An-ab**] = [**ab-Pe-An-ab**] = 2.0×10^{-5} M.

Fluorescence-lifetime measurements: Fluorescence lifetimes of the fluorophore-linked monomers and oligomers were measured to reinforce the above conclusions and are listed in Table 1. Single exponential decay was observed in the fluorescence-lifetime measurement of **7(Py)**, whereas fluorescence of the three pyrene-linked oligomers decayed double-exponentially. These two components can be interpreted to correspond to the monomer and

excimer emissions for the shorter lifetime (minor component) and the longer one (major component). Similar tendency was observed in the perylene-linked monomer and oligomer. However, in the case of **ab-An-An-ab**, the decay corresponding to its excimer could hardly be detected because the excimer emission is very weak, as shown in Figure 3B. Upon applying the heterooligomers, we used a cut-off filter (passing photons at >450 nm) to discard the photons emitted from the monomeric excited states in the oligomers. Thus, both the components observed for the heterooligomers must be assigned to fluorescence lifetimes from the heteroexcimers. This finding means that two or more conformational isomers emitted individually in agreement with their ground states deduced by the UV-visible spectra. Unfortunately, the emissive components in **ab-Py-Pe-Py-ab** were too numerous to be analyzed.

Conclusion

Our artificial DNA skeleton based on alkynyl *C*-nucleosides was found to be a superior scaffold for investigating homo- and heteroexcimer formation in aqueous media. The fluorescent oligomers made of the skeleton predominantly showed excimer emissions not only from homoexcimers but also from heteroexcimers. Because of the synthetic versatility of the alkynyl *C*-nucleosides, a large number of fluorophores can be attached to the skeleton. Therefore, these fluorophore-linked oligomers may be used for labeling various biomolecules, and such an approach is now underway.

Experimental Section

Synthesis of fluorescent oligomers: The fluorescent oligomers were synthesized from **5** by using an Applied Biosystems 392 synthesizer using standard β-cyanoethylphosphoramidite chemistry with the coupling reaction time of 15 min. The solid support (Universal Support II), which allows for 3′ placement of nonnatural nucleosides, was purchased from Glen Research. After automated synthesis, the oligomers were deprotected and removed from the solid support with 2-M ammonia methanol solution at room temperature for 30 min. The oligomers were then purified by reverse-phase HPLC by using a CHEMCOBOND 5-ODS-H column (10×150 mm with an eluent of 5×10^{-3} M ammonium formate and the following CH_3CN percentages of linear gradient (0–40 min) at a flow rate of 2.0 mL min^{-1}: **ab-Py-Py-ab** (20–45%), **ab-Py-Py-Py-ab** (30–60%), **ab-Py-Py-Py-Py-ab** (30–60%), **ab-Pe-Pe-ab** (30–50%), **ab-An-An-ab** (20–50%), **ab-Py-Pe-ab** (20–50%), **ab-Py-Pe-Py-ab** (30–60%), **ab-Py-An-ab** (20–40%), **ab-Pe-An-ab** (20–50%).

MALDI-TOF measurements: MALDI-TOF mass spectra were recorded by using a Bruker-Daltonics-Autoflex mass spectrometer with 3-hydroxypicolinic acid as a matrix. **ab-Py-Py-ab**: *m/z*: calcd for $C_{56}H_{54}O_{18}P_3$ [MH^+]: 1107.25; found: 1107.27, **ab-Py-Py-Py-ab**: *m/z*: calcd for $C_{79}H_{71}O_{23}P_4$ [MH^+]: 1511.33; found: 1511.10, **ab-Py-Py-Py-Py-ab**: *m/z*: calcd for $C_{102}H_{88}O_{28}P_5$ [MH^+]: 1915.41; found: 1915.09, **ab-Pe-Pe-ab**: *m/z*: calcd for $C_{64}H_{58}O_{18}P_3$ [MH^+]: 1207.28; found: 1206.87, **ab-An-An-ab**: *m/z*: calcd for $C_{52}H_{54}O_{18}P_3$ [MH^+]: 1059.25; found: 1059.31, **ab-Py-Pe-ab**: *m/z*: calcd for $C_{60}H_{56}O_{18}P_3$ [MH^+]: 1157.27; found: 1156.87, **ab-Py-Pe-Py-ab**: *m/z*: calcd for $C_{83}H_{73}O_{23}P_4$ [MH^+]: 1561.35; found: 1561.02, **ab-Py-An-ab**: *m/z*: calcd for $C_{54}H_{54}O_{18}P_3$ [MH^+]: 1083.25; found: 1082.99, **ab-Pe-An-ab**: *m/z*: calcd for $C_{58}H_{56}O_{18}P_3$ [MH^+]: 1133.27; found: 1132.92.

Spectroscopic measurements: Steady-state absorption and emission spectra were recorded by using a JASCO V-560 UV/Vis spectrophotometer and a JASCO FP-6500 spectrofluorometer, respectively. Fluorescence lifetimes were measured by using a HORIBA NAES-550 nanosecond fluorometer equipped with a SSU-111A photomultiplier, SCU-121A optical chamber, SGM-121A monochromator, and LPS-111 lamp power supply. These measurements were carried out at 25 °C using a 1-cm pathlength cell. Fluorescence quantum yields, Φ_f, of the monomers in H_2O were determined by using 9,10-diphenylanthracene[17] and perylene[18] as a standard with a known Φ_f in EtOH of 0.95 and 0.92, respectively. The fluorescence quantum yields were calculated according to the following equation: $\Phi_{f(spl)}=\Phi_{f(std)}\times[A_{std}/A_{spl}]\times[I_{std}/I_{spl}]\times[n_{std}/n_{spl}]^2$. In this equation, $\Phi_{f(spl)}$ and $\Phi_{f(std)}$ are the quantum yields of a sample and a standard, respectively. A_{spl}, I_{spl}, and n_{spl} are the optical density, the integrated emission intensity at the excitation wavelength, and the value of the refractive index of the sample, respectively. A_{std}, I_{std}, and n_{std} are those for the standard. Fluorescence lifetimes were obtained by time correction, a single-photon counting methodology, by means of a nanosecond fluorometer. Sample solutions (5.0×10^{-6} M) were prepared in Milli-Q water under aerated condition (not degassed). Excitation wavelengths were 275 nm (for **7**(**An**) and **ab-An-An-ab**), 350 nm (for **7**(**Py**), **ab-Py-Py-ab**, **ab-Py-Py-Py-ab**, **ab-Py-Py-Py-Py-ab**, **ab-Py-Pe-ab**, **ab-Py-An-ab**, **ab-Pe-An-ab**, and **ab-Py-Pe-Py-ab**), and 430 nm (for **7**(**Pe**) and **ab-Pe-Pe-ab**). Cut-off filters used were UV35 (for **7**(**Py**), **ab-Py-Py-ab**, **ab-Py-Py-Py-ab**, **ab-Py-Py-Py-Py-ab**, **7**(**An**), and **ab-An-An-ab**) and Y45 (for **7**(**Pe**), **ab-Pe-Pe-ab**, **ab-Py-Pe-ab**, **ab-Py-An-ab**, and **ab-Pe-An-ab**). All decay curves were calculated by using single or double exponential on the basis of the equation $I(t)=\Sigma A_i\exp(-t/\tau_i)$, in which $I(t)$ = fluorescence intensity at $t=0$, i = number of components, and A_i = fluorescence intensity of component i at $t=0$.

[1] a) B. Valeur, *Molecular Fluorescence*, Wiley-VCH, Weinheim, **2002**; b) H. Saigusa, E. C. Lim, *Acc. Chem. Res.* **1996**, *29*, 171–178.

[2] a) L. J. Johnston, B. D. Wagner in *Comprehensive Supramolecular Chemistry, Vol. 8* (Eds.: J. L. Atwood, J. E. D. Davies, D. D. MacNicol, F. Vögtle, J. A. Ripmeester), Pergamon, Oxford, **1996**, pp. 537–566; b) F. C. De Schryver, P. Collart, J. Vandendriessche, R. Geodeweeck, A. M. Swinnen, M. V. der Auweraer, *Acc. Chem. Res.* **1987**, *20*, 159–166. For recent letters and representative articles, see: c) C. Wang, Z. Wang, D. Zhang, D. Zhu, *Chem. Phys. Lett.* **2006**, *428*, 130–133; d) R. Karmakar, A. Samanta, *Chem. Phys. Lett.* **2003**, *376*, 638–645; e) C. A. van Walree, V. E. M. Kaats-Richters, L. W. Jenneskens, R. M. Williams, I. H. M. van Stokkum, *Chem. Phys. Lett.* **2002**, *355*, 65–70; f) D. Declercq, P. Delbeke, F. C. De Schryver, L. Van Meervelt, R. D. Miller, *J. Am. Chem. Soc.* **1993**, *115*, 5702–5708; g) K. Zachariasse, W. Kühnle, *Z. Phys. Chem. (Muenchen Ger.)* **1976**, *101*, 267–276.

[3] a) S. Wu, F. Zeng, H. Zhu, Z. Tong, *J. Am. Chem. Soc.* **2005**, *127*, 2048–2049; b) M. Belletete, E. Rivera, R. Giasson, X. X. Zhu, G. Durocher, *Synth. Met.* **2004**, *143*, 37–42; c) T. Nakano, T. Yabe, *J. Am. Chem. Soc.* **2003**, *125*, 15474–15484.

[4] a) F. Diederich in *Cyclophanes* (Ed.: J. F. Stoddart), The Royal Society of Chemistry, Cambridge, **1994**, pp. 1–51; b) H. Bouas-Laurent, J-P. Desvergne, F. Fages, P. Marsau in *Fluorescent Chemosensors for Ion and Molecule Recognition* (Ed.: A. W. Czarnik), American Chemical Society, Washington, **1992**, pp. 59–73; c) H. Abe, Y. Mawatari, H. Teraoka, K. Fujimoto, M. Inouye, *J. Org. Chem.* **2004**, *69*, 495–504; d) M. Inouye, K. Fujimoto, M. Furusyo, H. Nakazumi, *J. Am. Chem. Soc.* **1999**, *121*, 1452–1458; e) H. Langhals, R. Ismael, *Eur. J. Org. Chem.* **1998**, 1915–1917.

[5] a) C. J. Yang, S. Jockusch, M. Vicens, N. J. Turro, W. Tan, *Proc. Natl. Acad. Sci. USA* **2005**, *48*, 17278–17283; b) C. Honda, H. Kamizono, K. Matsumoto, K. Endo, *J. Colloid Interface Sci.* **2004**, *278*, 310–317; c) T. Ahn, J. S. Kim, H. I. Choi, C. H. Yun, *Anal. Biochem.* **2002**, *306*, 247–251; d) D. Sahoo, V. Narayanaswami, C. M. Kay, R. O. Ryan, *Biochemistry* **2000**, *39*, 6594–6601; e) S. A. V. Arman, A. W. Czarnik, *J. Am. Chem. Soc.* **1990**, *112*, 5376–5377; f) M. Zama, P. N. Bryan, R. E. Harrington, A. L. Olins, D. E. Olins, *Cold Spring Harbor Symp. Quant. Biol.* **1978**, *42*, 31–41.

[6] a) E. Mayer-Enthart, C. Wangner, J. Barbaric, H. A. Wagenknecht, *Tetrahedron* **2007**, *63*, 3434–3439; b) E. V. Bichenkova, A. R. Sardarian, A. N. Wilton, P. Bonnet, R. A. Bryce, K. T. Douglas, *Org. Biomol. Chem.* **2006**, *4*, 359–366; c) S. Nagatoishi, T. Nojima, B. Juskowiak, S. Takenaka, *Angew. Chem.* **2005**, *117*, 5195–5198; *Angew. Chem. Int. Ed.* **2005**, *44*, 5067–5070; d) K. Fujimoto, H. Shimizu, M. Inouye, *J. Org. Chem.* **2004**, *69*, 3271–3275; e) A. Okamoto, K. Kanatani, I. Saito, *J. Am. Chem. Soc.* **2004**, *126*, 4820–4827.

[7] a) R. Mejia, M. C. Gomez-Eichelmann, M. S. Fernabdez, *Biochem. Mol. Biol. Int.* **1999**, *47*, 835–844; b) T. Ahn, C. H. Yun, *J. Biochem.* **1998**, *124*, 622–627; c) A. Kölling, C. Maldonado, F. Ojeda, H. A. Diehl, *Radiat. Environ. Biophys.* **1994**, *33*, 303–313; d) B. W. van der Meew in *Subcellular Biochemistry, Vol. 13* (Eds.: H. J. Hilderson, J. R. Harris), Plenum, New York, **1988**, pp. 1–53.

[8] a) I. A. Prokhorenko, A. D. Malakhov, A. A. Kozlova, K. Momynaliev, V. M. Govorun, V. A. Korshun, *Mutat. Res.* **2006**, *599*, 144–151; b) K. J. Oh, K. J. Cash, K. W. Plaxco, *J. Am. Chem. Soc.* **2006**, *128*, 14018–14019; c) A. Cuppoletti, Y. Cho, J. S. Park, C. Strässler, E. T. Kool, *Bioconjugate Chem.* **2005**, *16*, 528–534; d) A. D. Malakhov, M. V. Skorobogatyi, I. A. Prokhorenko, S. V. Gontarev, D. T. Kozhich, D. A. Stetsenko, I. A. Stepanova, Z. O. Shenkarev, Y. A. Berlin, V. A. Korshun, *Eur. J. Org. Chem.* **2004**, 1298–1307; e) N. N. Dioubankova, A. D. Malakhov, Z. O. Shenkarev, V. A. Korshun, *Tetrahedron* **2004**, *60*, 4617–4626; f) S. M. Langenegger, R. Häner, *Chem. Commun.* **2004**, 2792–2793.

[9] a) J. Gao, S. Watanabe, E. T. Kool, *J. Am. Chem. Soc.* **2004**, *126*, 12748–12749; b) J. Gao, C. Strässler, D. Tahmassebi, E. T. Kool, *J. Am. Chem. Soc.* **2002**, *124*, 11590–11591; c) J. N. Wilson, J. Gao, E. T. Kool, *Tetrahedron* **2007**, *63*, 3427–3433.

[10] M. Takase, T. Morikawa, H. Abe, M. Inouye, *Org. Lett.* **2003**, *5*, 625–628.

[11] J. B. Birks, L. G. Christophorou, *Nature* **1962**, *194*, 442–444.

[12] H. Maeda, T. Maeda, K. Mizuno, K. Fujimoto, H. Shimizu, M. Inouye, *Chem. Eur. J.* **2006**, *12*, 824–831.

[13] F. M. Winnik, *Chem. Rev.* **1993**, *93*, 587–614.

[14] Even under indoor lighting, photosensitized oxidation gradually occurs on the perylene moiety in **7**(**Pe**) and **ab**-**Pe**-**Pe**-**ab**. Details for this unexpected reaction will be reported elsewhere.

[15] J. Tanaka, *Bull. Chem. Soc. Jpn.* **1963**, *36*, 1237–1244.

[16] a) A. Arnaud, J. Belleney, F. Boué, L. Bouteiller, G. Carrot, V. Wintgens, *Angew. Chem.* **2004**, *116*, 1750–1753; *Angew. Chem. Int. Ed.* **2004**, *43*, 1718–1721; b) A. Shimadzu, H. Ohtani, S. Ohuchi, K. Sode, M. Masuko, *Nucleic Acids Symp. Ser.* **1998**, *39*, 45–46.

[17] J. V. Morris, M. A. Mahaney, J. R. Huber, *J. Phys. Chem.* **1976**, *80*, 969–974.

[18] W. R. Dawson, M. W. Windsor, *J. Phys. Chem.* **1968**, *72*, 3251–3260.

Received: April 10, 2007
Published online: July 3, 2007

